Correlation of the internal fields, magnetic moments, and site preferences in $Fe_{3-x}Mn_xSi$ alloys*

V. Niculescu,† K. Raj, T. J. Burch, and J. I. Budnick

Physics Department and the Institute of Materials Science, The University of Connecticut, Storrs, Connecticut 06268

(Received 23 July 1975)

A detailed study of changes in the internal fields at Mn, Fe, and Si nuclei in the solid solutions of $Fe_{3-x}Mn_xSi$, $0 \leq x \leq 1.6$, as a function of composition has been made by spin-echo NMR at 1.28 K and in zero external magnetic field. Resonances due to Mn in three crystallographically different sites are observed. For $x < 0.75$, Mn enters predominantly the site with eight Fe first near neighbors and has an internal field of 259 kG shifted about 5.4 kG to lower values for each added Mn third near neighbor. For $x > 0.75$, Mn atoms also enter the other transition-metal site which has four Fe and Mn, and four Si first near neighbors and has an internal field of about 28 kG at $x = 0.75$. This field shifts to lower values as x increases. Mn enters the Si sites due to a small residual disorder of about 3% between Si and the Fe site with eight Fe first near neighbors. The internal field of Mn in these sites is about 127 kG at $x = 0.08$ and shifts slowly to higher values. The Fe and Si fields are compared with those in Fe_3Si alloys. The values of the internal fields and their variation with concentration at all sites are consistent with the magnetic moment and magnetization data of Yoon et al. Contributions to the internal fields from various neighbors are analyzed.

I. INTRODUCTION

It has been shown by spin-echo nuclear magnetic resonance[1] (NMR), and subsequently confirmed by neutron diffraction,[2] that *dilute* transition-metal impurities in Fe_3Si selectively enter one of the two inequivalent Fe sites. The site occupied depends on the position of the impurity in the Periodic Table. Furthermore, it has been noted that a definite relationship exists between the site selected by a dilute impurity in Fe_3Si and the site it occupies in Heusler alloys. It thus appears that a detailed study of hyperfine interactions in Fe_3Si at *higher* impurity concentrations could provide valuable information on the mechanisms responsible for site preference.

The system $Fe_{3-x}Mn_xSi$ is very suitable for this purpose because it forms a continuous range of solid solutions with the same crystalline structure and provides an opportunity to investigate magnetic behavior as a function of environment. In this system one passes from the binary Fe_3Si, which is ferromagnetic, to the Heusler Fe_2MnSi with a complex spin structure,[3] and finally to Mn_3Si. Moreover, the neutron diffraction study of Yoon et al.[3] provides information on Mn site occupation, magnetic moments, and magnetic structure over the composition range $0 \leqslant x \leqslant 1.75$.

In this paper we report a detailed study of the hyperfine interactions for the Mn, Fe, and Si sites in the $Fe_{3-x}Mn_xSi$ system and obtain valuable information on the crystallographic and magnetic structure of this system. Most emphasis will be placed on the Mn and Fe results.

The present study enables us to (i) further explore the selective site mechanism by determining the concentration limits of the selectivity, (ii) determine directly the dependence of the local Mn moment and hyperfine field on the various environments possible throughout the composition range studied in this paper, and (iii) further explore the conduction-electron polarization effects in a unique manner made possible by the nature of the host and the extreme substitutional selectivity of the Mn. The behavior of the field data with concentration will be interpreted in light of the neutron studies of Yoon et al.[3] in an effort to further understand the complex magnetic behavior which begins to set in at about $x = 0.75$.

II. $Fe_{3-x}Mn_xSi$ SYSTEM

In Fig. 1, a unit cell describing the $Fe_{3-x}Mn_xSi$ system is shown. In referring to atoms occupying sites in this lattice we will write the lattice sites A, B, C, and D in parentheses. Thus for Fe on a B site we will use $Fe(B)$.

Fe_3Si is a well-ordered intermetallic ferromagnet with a Curie temperature of 803 K. In this compound, with DO_3 crystal structure, there are two inequivalent Fe sites, namely, $Fe(B)$ and $Fe(A, C)$, and a $Si(D)$ site with the neighbor configurations shown in Table I. In the notation used here the formula Fe_3Si becomes $[Fe(A, C)]_2Fe(B)$ $\times Si(D)$. The magnetic moments on the $Fe(B)$ and $Fe(A, C)$ sites are $2.3\mu_B$ and $1.4\mu_B$, respectively.[4]

The existing data on Mn site occupation and the site magnetic moments in $Fe_{3-x}Mn_xSi$ as functions of Mn concentration are presented in Figs. 2 and 3, respectively.
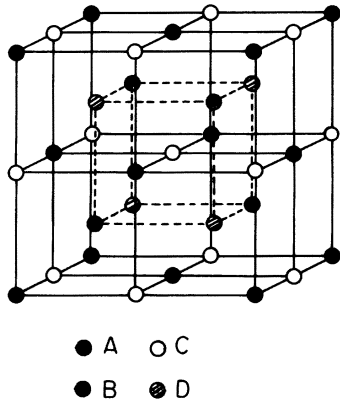
FIG. 1. Unit cell of $Fe_{3-x}Mn_x$ Si alloy system. The sites are represented by A, B, C, and D. The A and C sites are equivalent and together with the B sites are occupied by Fe and/or Mn depending on the alloy concentration. The D site is occupied by Si.

FIG. 2. Filling of A, C, and B sites with Mn as a function of concentration (x) in $Fe_{3-x}Mn_x$ Si. The data points (x) were obtained from the NMR spectra of the Mn(B) site (see text).

Small amounts of Mn added to Fe_3Si enter the B sites.[1,2] The neutron diffraction data[3,5] show that Mn enters the B site for Mn concentrations between $x = 0$ and $x = 0.75$. Throughout this composition range $Fe_{3-x}Mn_x$Si remains a ferromagnet with T_C decreasing to 370 K. The average moment on the B site remains constant indicating that Mn(B) has a moment approximately equal to that of Fe(B), viz., $2.3(3)\mu_B$. The moment of the A and C sites, which contain only Fe(A, C), decrease from $1.4\mu_B$ to $0.3\mu_B$ as x increases from 0 to 0.75. Furthermore, Yoon et al.[3] find that in alloys with $x > 0.75$ Mn begins to enter the A and C sites. At $x \simeq 1$ about 85% of the Mn atoms are on B sites and about 15% on A and C sites.[5] At $x = 1.5$ the B sites were found to be completely filled with Mn.[6] For compositions $0.75 \leqslant x \leqslant 1.75$, $Fe_{3-x}Mn_x$Si is ferromagnetic above about 77 K. Below 77 K the neutron diffraction data suggested the presence of rhombohedral antiferromagnetic ordering. The B

site moment, in the range $0.75 \leqslant x \leqslant 1.75$, falls gradually to zero while the A and C site moment remains practically constant up to $x \simeq 1.5$ and then decreases gradually to zero.

III. SAMPLE PREPARATION

All alloys used in these studies were formed by arc melting appropriate proportions of high-purity (99.99%) iron, silicon, and manganese in an argon atmosphere. Samples for $x = 0$, 0.08, 0.15, 0.25, 0.50, 0.65, 0.75, 1.0, 1.25, 1.50, 1.60, and 1.75 were made. The weight loss in all the samples was close to 1%.

These ingots were heated in a quartz tube to about 200°C for 2 h in vacuum and then sealed off under pressure of the order of 6×10^{-6} Torr. The sealed tubes were then annealed at 800°C for 24 h and slowly cooled from 800 to 600°C at a rate of

TABLE I. $Fe_{3-x}Mn_x$ Si neighbor configurations.

No. of shell	1	2	3	4	5	6	7	8
Neighbor distance in lattice parameters	0.43	0.5	0.705	0.83	0.86	1	1.08	1.11
A, C	$4B$ $4D$	$6A, C$	$12A, C$	$12B$ $12D$	$8A, C$	$6A, C$	$12B$ $12D$	$24A, C$
B	$8A, C$	$6D$	$12B$	$24A, C$	$8D$	$6B$	$24A, C$	$24D$
D	$8A, C$	$6B$	$12D$	$24A, C$	$8B$	$6D$	$24A, C$	$24B$
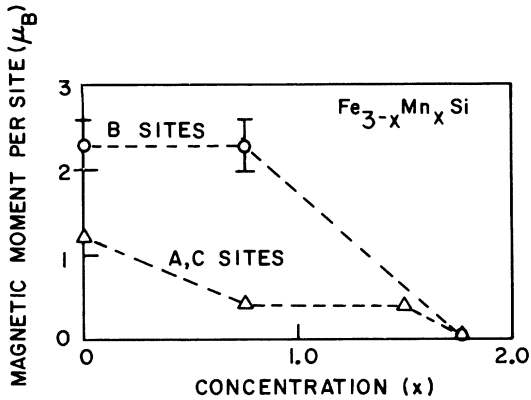
FIG. 3. Variation of A, C, and B site's magnetic moment as a function of concentration (x). The data are those of Yoon et al. (Ref. 3). We have assumed a linear extrapolation between the data points.

40°C/h. Finally the samples were water quenched from 600°C.

The ingots were powdered to No. 400 mesh. The powder was annealed at 600°C for 1 h under vacuum $(2 \times 10^{-6}$ Torr) and cooled to room temperature in about 2 h. X-ray analysis showed that the powdered samples were single phase and were well ordered.

IV. EXPERIMENTAL RESULTS

A. Structural characteristics

X-ray data on $Fe_{3-x}Mn_xSi$ alloys were taken with a Philips diffractometer using Cu K_α radiation. The lattice parameters were obtained by extrapolation to $\theta = 90°$ for the parameters corresponding to the fundamental lines (440), (620), and (444) for both $K\alpha_1$ and $K\alpha_2$ radiation. In Fig. 4, we have shown the variation of lattice constant with Mn concentration. The results are in a good agreement with previous studies.[3,7] No evidence of a second phase was found for the experimental conditions used in these studies. A direct determination of the long-range order was carried out for several of the samples. The unit cell (Fig. 1) for these alloys can be described in terms of four interpenetrating fcc sublattices A, B, C, D with origins at $A(0,0,0)$, $B(\frac{1}{4}, \frac{1}{4}, \frac{1}{4})$, $C(\frac{1}{2}, \frac{1}{2}, \frac{1}{2})$, and $D(\frac{3}{4}, \frac{3}{4}, \frac{3}{4})$. For this structure only those Bragg reflections are allowed for which Miller indices are either all odd or all even. This gives rise to the following three types of structure amplitudes:

(i) $F_1 \sim [(f_A - f_C)^2 + (f_B - f_D)^2]^{1/2}$ corresponding to the odd values of hkl for the superlattice lines (111), (311), (331), (511), (333), (531);

(ii) $F_2 \sim (f_A - f_B + f_C - f_D)$ corresponding to $h + k + l = 2n$ (n is an integer) for the superlattice lines
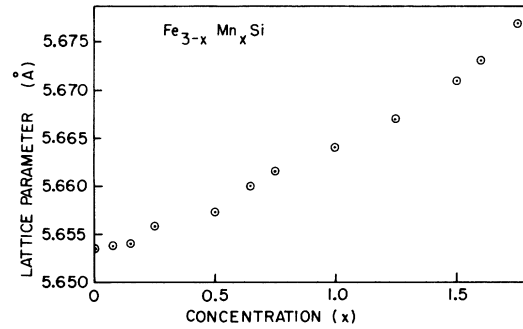
FIG. 4. Variation of lattice parameter as a function of concentration (x) in $Fe_{3-x}Mn_x Si$.

(200), (222), (420);

(iii) $F_3 \sim (f_A + f_B + f_C + f_D)$ corresponding to $h + k + l = 4n$ for the fundamental lines (220), (400), (422), (400), (620), (444).

Here f_A, f_B, f_C, and f_D are the average scattering factors for A, B, C, and D sites, respectively.

In order to get some numerical estimate of the degree of disorder in $Fe_{3-x}Mn_xSi$, a sample of Fe_3Si was first measured. In well-ordered Fe_3Si, A, B, and C sites are occupied by Fe atoms and D sites by Si atoms. The structure amplitudes for this alloy are given by

$$F_1 \sim (f_{Fe} - f_{Si}), \quad F_2 \sim (f_{Fe} - f_{Si}), \quad F_3 \sim (f_{Fe} + f_{Si}),$$

so that the ratio $F^2_{(111)}/F^2_{(200)} = 1$.

For a completely ordered Fe_3Si, the neighbor configurations are shown in Table I. Some disorder between Fe and Si sites would introduce a corresponding change in specific near-neighbor (nn) shells. Let α and β be the fractions of $Fe(B)$ and $Fe(A,C)$ atoms, respectively, which occupy Si sites. Then

$$\frac{F^2_{(111)}}{F^2_{(200)}} = \frac{(1 - 2\alpha - \beta)^2}{(1 - 2\beta)^2}.$$

By assuming $\beta = 0$, about 3% of disorder between the $Fe(B)$ and Si sites per formula unit was found, in good agreement with recent neutron results on a similarly prepared Fe_3Si sample.

The order parameter for Fe_3Si is easy to obtain since Fe and Si have different atomic scattering factors. The problem is more complex in $Fe_{3-x}Mn_xSi$ since Fe and Mn have nearly the same scattering factors. This fact combined with absorption corrections makes it extremely difficult to deduce the amount of Fe-Mn disorder from x-ray data alone. One can still, however, determine the disorder between the B sites (Fe and Mn) and Si.

For all the concentrations studied between Fe_3Si and Fe_2MnSi, we find from the x-ray data that the

ratios $F^2_{(111)}/F^2_{(220)}$ and $F^2_{(200)}/F^2_{(220)}$ remain essentially the same and that $F^2_{(111)}/F^2_{(200)}$ has the same value as for Fe_3Si. If we again set $\beta = 0$, we conclude that in all the samples a degree of disorder $\alpha = (3 \pm 1)\%$ between the B and D sites exists. This disorder has been independently verified by neutron diffraction experiments.[2]

B. Hyperfine-field results

The NMR spectra were measured by using a spin-echo technique described elsewhere.[8] All the resonances reported here were measured at 1.28 K and in zero external magnetic field.

The spin-echo spectra of these alloys will be discussed in terms of three frequency ranges. Spectral lines between 200 and 300 MHz are assigned to Mn on B sites. Lines between 110 and 160 MHz which are observed in samples with $x \leqslant 1.0$ are identified as Mn in D sites. Lines between 10 and 60 MHz are due to Fe on B sites, Fe on A and C sites, and Si on D sites in alloys with $x \leqslant 0.75$. In alloys with $x \geqslant 0.75$ a strong contribution from Mn atoms in A and C sites is found in this frequency range.

1. High-frequency spectra: Mn(B) sites

In Fig. 5, we show a plot of echo amplitude vs frequency for frequencies between 200 and 300 MHz. These spin-echo signals are due to Mn nuclei in the B sites. This identification as Mn in B sites was originally made for dilute Mn substitutions.[1] The structure and intensity of the satellites is inconsistent with any other assignment.

For $x = 0.08$, 0.15, and 0.25, the several well-resolved neighbor satellites are assigned to Mn atoms with varying numbers of Mn in the third-neighbor shell. At the main Mn line (labeled 0) the internal field is about 259 kG for $x = 0.08$, the most dilute sample studied here. The sign of this field has not yet been determined. This Mn site has twelve Fe and zero Mn third nn. For small increases in Mn, the frequency of this line shifts to higher values as shown in Fig. 6. Each added Mn in this dilute range produces a shift ΔH at the Mn(B) site of about 5.7 kG corresponding to the negative frequency shift of 6.0 MHz. The concentration dependence of the line positions corresponding to all the peaks observed is also shown in Fig. 6. A systematic increase in frequency with increasing Mn concentration is observed for all peaks resolved for $x \leqslant 0.25$. The relative intensities of the satellites for $x \leqslant 0.25$ are consistent with a random distribution of Mn atoms on B sites.

The internal field at the Mn nuclei can be described in terms of a sum of three main contributions:
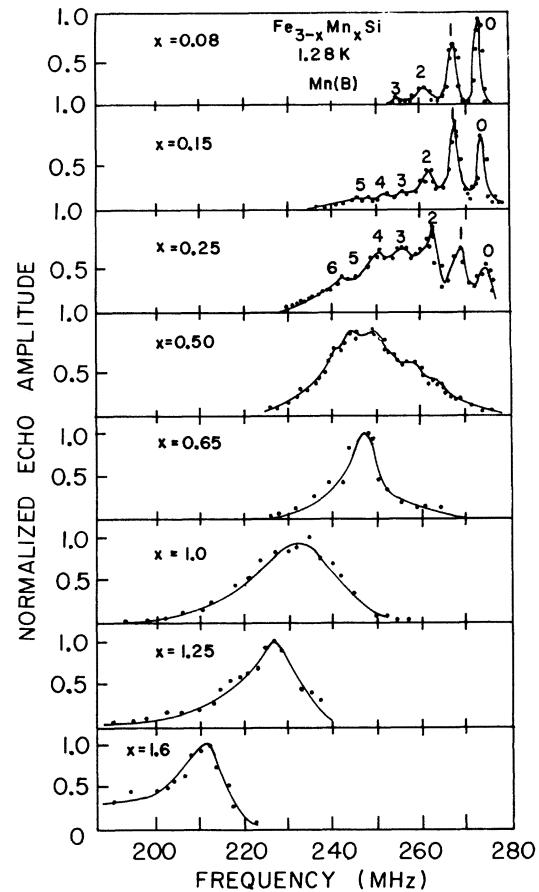
FIG. 5. Spin-echo spectra of ^{55}Mn nuclei on B site in $Fe_{3-x}Mn_xSi$ alloys from $x = 0.08$ to 1.6.

$$H_{Mn} = H_{CP} + H_s + H_{CEP},$$

where H_{Mn} is the internal field observed at the Mn nuclei, H_{CP} is the core polarization, H_s is the polarization of the s-like conduction electrons on the atom itself, and H_{CEP} is the conduction-electron polarization (CEP) produced by all the Fe and Mn in the neighboring shells.

For $x \leqslant 0.25$ each added Mn in the third-neighbor shell produces approximately the same shift of about 2.1%. The approximate linearity extending to five or more Mn substitutions in the third-nn shell strongly suggests that shifts produced are mainly the result of changes in conduction-electron polarization. Throughout this range the Mn moment is found to remain constant[3]—an observation entirely consistent with the dominance of perturbations in only the CEP produced by these Mn in the third-nn shell. The shift per added Mn is shown to decrease with increasing Mn substitution. (See insert Fig. 6.)

For $x > 0.25$ less-well-resolved satellites are observed at the resolution used in these experiments.
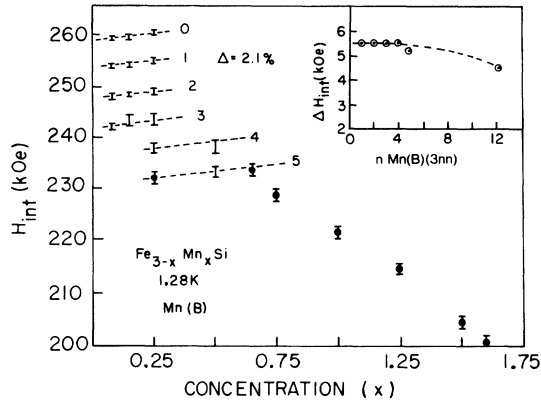
FIG. 6. Concentration dependence of the [55]Mn internal fields at the B sites. The numbers 0 to 5 are used to identify the fields of Mn(B) which have 0 to 5 third-nn Mn atoms. The points for $x > 0.50$ indicate the field corresponding to the maximum intensities of the line. The insert shows the shift in the Mn(B) internal field as a function of the number of Mn third nn.

There is, however, a steady shift in the center of gravity of the spectrum as well as a pronounced and growing asymmetry for $x > 0.75$. This relatively small shift in the Mn internal field is to be contrasted with the reduction of the average Fe(B) and Mn(B) site moment deduced from Yoon's neutron work as shown in Fig. 3. This contrast can be understood if we postulate that some of the Mn moments align themselves antiparallel to each other or to the average B site moment. The local behavior of the Mn(B) site relative spin alignment deduced from spin-echo results is also consistent with the observed reduction in the saturation magnetization at low temperatures in this concentration range. The pronounced asymmetry seen in the spectra for $x > 0.75$ is caused by Mn atoms now entering the A and C sites. Thus some of the Mn(B) sites will have Mn(A, C) as first nn. The reduction in the internal field at those Mn(B) sites with Mn(A, C) first nn is about 6%. This number, although approximate, is obtained by decomposing the lines into two symmetric contributions. The relative intensity of these lines is in agreement with the fractional occupation of Mn in the A, C sites as shown in Fig. 2. A steady increase in rf power, compared to that needed at low concentration, is required to excite echoes for x above about 0.75. This observation suggests a decrease in rf enhancement factor consistent with a change in spin structure deduced from magnetization measurements. A reduction in enhancement factor is also consistent with the onset of some type of more complex spin order above $x = 0.75$. Owing to transmitter limitations no spin echoes were observed in samples with $x > 1.60$.

2. Low-frequency spectra: Fe(B), Fe(A,C), Si(D), and Mn(A,C) sites

Our spectral results for the frequency range 16–50 MHz are shown in Fig. 7. The top spectrum is for well-ordered Fe_3Si.[1,9] The positions of the observed lines are indicated by vertical bars; their linewidths, which are less than 100 kHz, cannot be shown in the scale used for this figure. The lines at 46.67 and 30.07 MHz are from Fe nuclei at Fe(B) and Fe(A, C) sites, respectively. The line at 31.2 MHz is due to Si nuclei on D sites.

As Mn is added, clear structure is seen on the spectra of the Fe(B) site and the Si site for $x = 0.08$, $x = 0.15$, and $x = 0.50$. Some structure also occurs in the Fe(A,C) field distribution. In the low-concentration range Mn substitutes into the third-neighbor shell and produces shifts in the Fe(B) field of 2.5% (Fig. 8). These shifts are nearly the same as those produced by Mn third neighbors on the Mn(B) field. Pure conduction-electron polarization effects for the third-nn shell would account for such scaling of the Fe(B) and Mn(B) spectra.[10] Here again as seen in Table I,
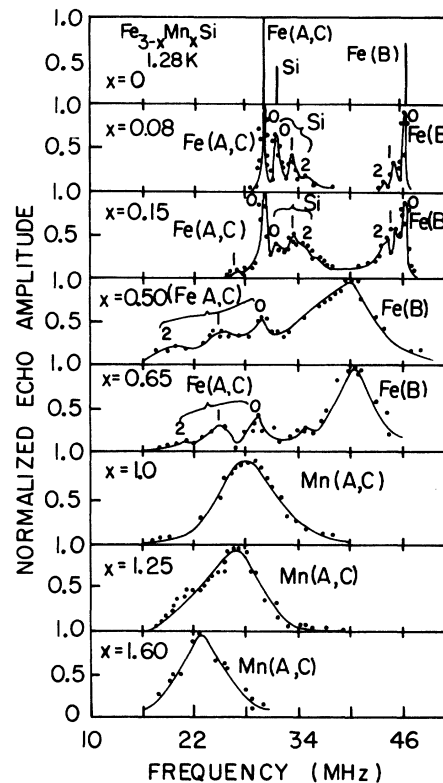
FIG. 7. Spin-echo spectra of $Fe_{3-x}Mn_x$ Si alloys in the low-frequency range. See the text and the labels in the figure for the identification of Fe(A, C), Fe(B), Si(D), and Mn(A, C) lines.
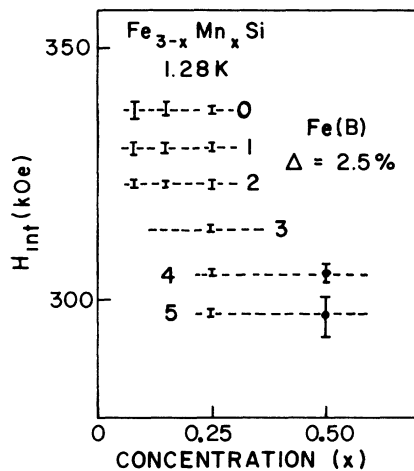
FIG. 8. Concentration dependence of the internal field at the ^{57}Fe nuclei in the B site. The numbers 0 to 5 are used to identify the fields of Fe(B) which have 0 to 5 third-nn Mn atoms.

the Fe_3Si structure provides us with a special situation in which to carefully study CEP effects associated with specific distant-neighbor shells. The large number of different contributions in this low-frequency spectra make it difficult to resolve the Fe(B) internal field above $x = 0.50$. The total observed change in the Fe(B) internal field is 14.8% from $x = 0$ to $x = 0.75$ and this is consistent with the reported B site moment behavior in this concentration range.[3,5]

The higher-frequency satellites observed in the Si spectrum for $x = 0.08$ and 0.15 are due solely to Mn substitutions into the second-nn shell about the Si (see Fig. 7 for identification). For $0 \leq x \leq 0.75$ Mn substitution into B sites changes the first-nn configurations of the Fe(A, C) sites. The observed satellites occur at frequencies which are about 18% lower than the main line, reflecting the strong field perturbation brought about by the first-nn Mn substitution. The neutron diffraction results show that a strong reduction in the Fe(A, C) site moment occurs but that the average B site moment remains constant in this concentration range (see Fig. 3). Thus we can conclude that the 18% shift in the internal field of Fe(A, C) is due to a change in H_{CP} connected with a strong configurational perturbation of the Fe(A, C) local moment by Mn neighbors.

A comparison of the low-frequency NMR spectra with Mössbauer results[11] proves that an additional Mn contribution is observed in this low-frequency range for $x \geq 0.75$. The observation of increasing NMR intensity in this low-frequency range can only be consistent with the identification of a signal at this region of the spectrum with Mn. At higher concentrations, e.g., above $x = 0.75$, the indicated

intensity is essentially due to Mn in the A and C sites. Most of the Mn(A, C) sites in this concentration range have four Mn(B) and four Si(D) as first NN. The Mn(A, C)-Mn(B) interaction leads to a spin reorientation for the Mn(B) sites and a decrease in the value of magnetic moments of Mn(A, C) and therefore in H_{CP}(Mn).

The internal field at this Mn site for $0.75 \leq x \leq 1.6$ ranges between 28 and 21 kG, consistent with the low moments deduced from the neutron diffraction studies. Such low values for a Mn internal field have been observed in[12] α-Mn for a site commonly labeled III. These sites have an internal field of 25.2 kG and a corresponding magnetic moment of $0.6\mu_B$ at 4.2 K.

For $x \geq 0.75$ the frequency decreases at these Mn(A, C) sites reflecting the large increase in Mn substitutions into the second- and third-neighbor shells. (See Table I.)

All of our spectral analyses have been confined to substitutions up to the third-nn shell. More distant neighbor configurations would have some effect on the line shape and linewidth but are not expected to influence the analysis and conclusions presented here.
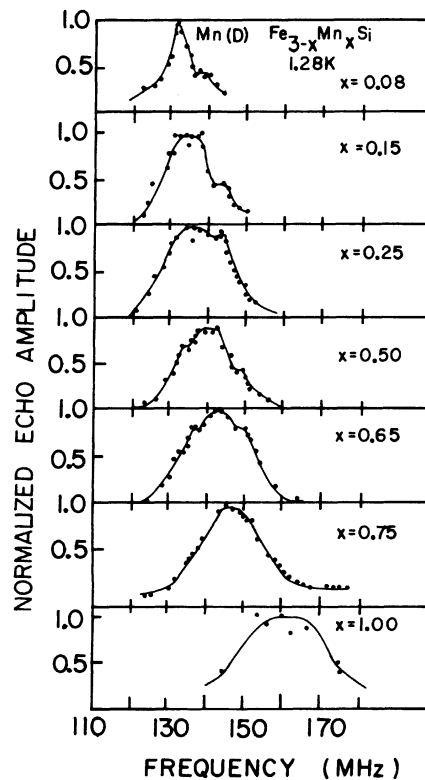
FIG. 9. Spin-echo spectra of ^{55}Mn nuclei on D sites in $Fe_{3-x}Mn_x Si$ alloys for compositions from $x = 0.08$ to 1.0.

3. Midfrequency spectra: Mn(D) sites (the effect

of residual disorder)

In all samples studied as well as in Fe_3Si we have already noted that there is a small degree of disorder between B and D sites. A careful study of our samples showed a line whose dependence on concentration is shown in Fig. 9. This line is very weak and has an intensity of about 3% of that of the $Mn(B)$ line. The degree of disorder found between B and D sites is consistent with assigning this resonance to Mn in the D sites. The value of the hyperfine field at a $Mn(D)$ site having no Mn in the second-nn shell is about 127 kG and slowly shifts to higher values with increasing x.

V. SUMMARY AND CONCLUSIONS

The correlation of these extensive NMR results with neutron diffraction, magnetization, and Mössbauer data enables us to see clearly the dependence of the internal field on the specific environments and to understand in detail the local moment behavior. Clear evidence for CEP effects are demonstrated in this system for third-neighbor substitutions on both $Mn(B)$ and $Fe(B)$ sites.

This study supports the strong preference for the Mn in the site with eight Fe first nn up to about $x = 0.75$, as determined by the neutron diffraction work.[2,3] This selectivity is consistent with recent work on dilute Fe-based alloys which show clear evidence for Mn-Mn repulsion.[13] The Mn substitution into the Si site can be understood on the basis of residual disorder measured by x rays and confirmed by the neutron diffraction studies.[6]

Above $x > 0.75$, we see clear evidence for Mn entering the A, C sites. The population of this site by Mn with increasing x determined from the NMR data bears out the trend expected from the neutron diffraction results as shown in Fig. 2.

By comparing the NMR results on the $Mn(A,C)$ sites with neutron diffraction results we conclude that a local antiparallel pairing of first-nn Mn moments occurs for $x > 0.75$. This provides another basis for understanding the onset of the complex magnetization behavior observed in both

the bulk magnetization and neutron diffraction data.

For low concentrations, the intensities of the $Mn(B)$ and $Fe(B)$ spectra are consistent with a random substitution of Mn into the B sites. The observed satellites for both these lines largely reflect changes in the CEP.

The substitution of Mn into a distant specific neighbor shell, made possible in the Fe_3Si lattice, eliminates chemical and direct environment effects normally present in dilute-alloy studies, where a first-nn impurity can drastically affect a moment or the hyperfine coupling constant. The Mn spectra show clearly satellite structure associated with predominantly third-nn substitutions. The hyperfine-field shift of these satellites to a high degree is linearly dependent on the number of substituted Mn up to $n = 5$ and possibly for larger n. The Fe signal also allows clear resolution of the CEP effects produced by the addition of Mn to its third-nn shell.

Large differences exist for the $Mn(B)$, $Mn(A, C)$, and $Mn(D)$ hyperfine fields which we have associated with well-defined Mn sites with specific near-neighbor environment. The large differences in the Mn hyperfine fields observed for the different Mn sites is consistent with the moment variation deduced from the neutron diffraction experiment.

Detailed magnetic moment values for the specific sites observed in the NMR spectra have not yet been determined.

ACKNOWLEDGMENTS

---

[1]T. J. Burch, T. Litrenta, and J. I. Budnick, Phys. Rev. Lett. **33**, 421 (1974).

[2]S. Pickart, T. Litrenta, T. Burch, and J. I. Budnick, Phys. Lett. A **53**, 321 (1975).

[3]S. Yoon and J. G. Booth, Phys. Lett. A **48**, 381 (1974); J. G. Booth, J. E. Clark, J. D. Ellis, P. J. Webster, and S. Yoon, in *Proceedings International Conference on Magnetism, Moscow, 1973* (Nauka, Moscow, 1974), Vol. IV, p. 577.

[4]A. Paoletti and L. Passari, Nuovo Cimento **32**, 1449 (1964).

[5]S. Pickart (private communication).

[6]J. G. Booth (private communication).

[7]E. I. Gladysevskij, Fiz. Met. Metalloved. $\underline{2}$, 454 (1956).

[8]J. I. Budnick and S. Skalski, *Hyperfine Interactions*, edited by A. J. Freeman and R. Frankel (Academic, New York, 1967), pp. 724–36.

[9]M. B. Stearns, Phys. Rev. $\underline{129}$, 1136 (1963).

[10]M. Rubinstein, G. H. Stauss, and J. Dweck, Phys. Rev. Lett. $\underline{17}$, 1001 (1966).

[11]R. Frankel (private communication).

[12]H. Yamagata and K. Asayama, J. Phys. Soc. Jpn. $\underline{33}$, 400 (1972).

[13]Le Dang Khoi, P. Veillet, and I. A. Campbell (private communication).